

Locality of correlation in density functional theory

Kieron Burke, Antonio Cancio, Tim Gould, and Stefano Pittalis

Citation: *The Journal of Chemical Physics* **145**, 054112 (2016); doi: 10.1063/1.4959126

View online: <http://dx.doi.org/10.1063/1.4959126>

View Table of Contents: <http://scitation.aip.org/content/aip/journal/jcp/145/5?ver=pdfcov>

Published by the *AIP Publishing*

Articles you may be interested in

[Global and local curvature in density functional theory](#)

J. Chem. Phys. **145**, 054109 (2016); 10.1063/1.4959882

[Reduced density-matrix functional theory: Correlation and spectroscopy](#)

J. Chem. Phys. **143**, 024108 (2015); 10.1063/1.4926327

[Comparing ab initio density-functional and wave function theories: The impact of correlation on the electronic density and the role of the correlation potential](#)

J. Chem. Phys. **135**, 114111 (2011); 10.1063/1.3636114

[Density functional theory for pair correlation functions in polymeric liquids](#)

J. Chem. Phys. **114**, 4323 (2001); 10.1063/1.1348031

[Analysis of dynamical and nondynamical components of electron correlation energy by means of local-scaling density-functional theory](#)

J. Chem. Phys. **106**, 9227 (1997); 10.1063/1.474024



NEW Special Topic Sections

NOW ONLINE
Lithium Niobate Properties and Applications:
Reviews of Emerging Trends

AIP | Applied Physics
Reviews

Locality of correlation in density functional theory

Kieron Burke,¹ Antonio Cancio,² Tim Gould,³ and Stefano Pittalis⁴

¹Department of Chemistry, University of California, Irvine, California 92697, USA

²Department of Physics and Astronomy, Ball State University, Muncie, Indiana 47306, USA

³Qld Micro- and Nanotechnology Centre, Griffith University, Nathan, Qld 4111, Australia

⁴CNR-Istituto di Nanoscienze, Via Campi 213A, I-41125 Modena, Italy

(Received 27 February 2016; accepted 5 July 2016; published online 3 August 2016)

The Hohenberg-Kohn density functional was long ago shown to reduce to the Thomas-Fermi (TF) approximation in the non-relativistic semiclassical (or large- Z) limit for all matter, i.e., the kinetic energy becomes local. Exchange also becomes local in this limit. Numerical data on the correlation energy of atoms support the conjecture that this is also true for correlation, but much less relevant to atoms. We illustrate how expansions around a large particle number are equivalent to local density approximations and their strong relevance to density functional approximations. Analyzing highly accurate atomic correlation energies, we show that $E_C \rightarrow -A_C Z \ln Z + B_C Z$ as $Z \rightarrow \infty$, where Z is the atomic number, A_C is known, and we estimate B_C to be about 37 mhartree. The local density approximation yields A_C exactly, but a very incorrect value for B_C , showing that the local approximation is less relevant for the correlation alone. This limit is a benchmark for the non-empirical construction of density functional approximations. We conjecture that, beyond atoms, the leading correction to the local density approximation in the large- Z limit generally takes this form, but with B_C a functional of the TF density for the system. The implications for the construction of approximate density functionals are discussed. *Published by AIP Publishing.* [<http://dx.doi.org/10.1063/1.4959126>]

I. INTRODUCTION

Kohn-Sham (KS) density functional theory¹ (DFT) enjoys remarkable popularity, being used in more than 30 000 papers last year.² Essentially all these calculations use some approximation to the exchange-correlation energy, E_{XC} , as a functional of the (spin)-densities.³ Although many hundreds of such approximations exist and appear in standard codes, most calculations are run with one of a few approximations. These standard approximations^{4–8} have been around for almost twenty years and their successes and failures are well-known. Of course there are many excellent improvements beyond these approximations for specific purposes.^{9,10}

Although the exact theory of DFT is well-established^{11,12} and rarely questioned these days, it is sometimes claimed that there is no systematic approach to the overall construction of approximate functionals. In fact, this is not true. More than 40 years ago, Lieb and Simon (LS) proved that Thomas-Fermi (TF) theory becomes relatively exact for the total (non-relativistic) energy of any system in a limit in which both the particle number N becomes large and the coordinates are scaled. For atoms, this amounts to $Z \rightarrow \infty$, where Z is the nuclear charge, while keeping the atom neutral ($Z = N$). But the limit also applies to all molecules and solids, once their bond lengths are simultaneously scaled.¹³ This limit then implies a systematic approach to the construction of density functionals, by finding the density functional corrections to the TF approximation that yield the exact leading corrections to the TF energy. Unfortunately, even in very simple situations, deriving and using these leading corrections can be very demanding, and they will not, in general, be explicit

density functionals.^{14–16} Nonetheless, such functionals are, in principle, well-defined, if not easily approximated.

The modern world uses the KS variant of DFT, in which only the XC energy needs approximating. Schwinger demonstrated^{17,18} that, for atoms, the local density approximation (LDA) for exchange becomes relatively exact in the large- Z limit, and a proof (for non-singular potentials) was given by Conlon in the general case.¹⁹ A rigorous proof for atoms was given by Fefferman and Seco.²⁰ The next correction was estimated by Elliott and Burke²¹ and shown to be accurately reproduced by both the B88 functional⁴ and the exchange part of PBE.⁸ Thus, at the generalized gradient approximation (GGA) level, the most commonly used approximations (at least 70% of present calculations²) reproduce the leading correction to LDA in this limit. This insight was used (in an inverted piece of logic) to construct the exchange functional in PBEsol,²² which is useful for calculating the equilibrium properties of solids (but not their thermochemistry). The tension between accurate energetics and bond lengths^{23,24} suggests that the GGA form is insufficient to capture all aspects of the leading correction to LDA accurately.²² The asymptotic expansion for exchange has been used to construct new functional approximations.^{25–27}

The present paper explores the next logical step in this analysis: Does the correlation energy alone also become relatively exact in LDA in this limit? If so, what is the leading correction, and do standard approximations capture this? These are very fundamental questions about the nature of the XC functional and our ability to approximate it with semilocal functionals. Such questions concern properties of the exact functional that are highly relevant to approximations.

We cannot hope to answer this question in general at present, but we can try to answer this question in the one case where we have sufficient data: atoms. By very carefully analyzing accurate correlation energies²⁸ for a sequence of non-relativistic atoms up to $Z = 86$, we find that they can be fitted to the following form:

$$E_C \rightarrow -A_C Z \ln Z + B_C Z. \quad (1)$$

The first constant, A_C , is about 20.7 mhartree and is derived from the uniform electron gas and confirmed analytically in Ref. 29. The second constant, B_C , is a property of all atoms and is highly *inaccurate* in LDA. From theory and our calculations, we estimate B_C to be 37.2 mhartree, whereas in LDA, it is found analytically to be -4.5 mhartree. However, even this very limited information yields much insight into the nature of the correlation energy functional. At a very elementary level, we see why it has been so much more difficult to identify than the exchange form: the $1/|\mathbf{r} - \mathbf{r}'|$ behavior of the Coulomb potential produces a $Z \ln Z$ term, so that only at astronomical values of Z does the LDA correlation become relatively exact. The fact that B_C^{LDA} is negative helps to explain the huge overestimate of LDA correlation energies. We also note that it is *only* the high-density limit of LDA that is relevant to atoms, not the entire density dependence of the uniform gas. Thus, within this analysis, the LDA is only particularly relevant for Coulomb matter in the extreme high-density limit. Of course, for a simple valence metal solid which is well-approximated by a uniform gas, the LDA is needed to produce an accurate correlation energy. Moreover, for energy differences and derivatives with respect to nuclear coordinates that are relevant to bond lengths, more terms in the LDA correlation energy might be relevant.

A first modern attempt to extract the behavior of the correlation energies for large non-relativistic atoms was made by Kunz and Rueedi.²⁹ They complemented analytical work based on a perturbative many-body approach with numerical values from Clementi and Corongiu³⁰ up to $Z = 54$. Their estimate for B_C is inaccurate, due to inaccuracies in the data and an insufficiently precise extrapolation.³¹

The layout of this article is a little unusual. Almost half of the material is introductory, explaining how the Lieb-Simon limit is relevant to approximating density functionals for any component of the energy: kinetic, exchange, or correlation. This is needed to understand the relevance of the results for correlation. Part of doing this is a simple illustration of how the large- N limit of a series can be used to accurately approximate its value for *all* values of N , including even $N = 1$ (or less). We also use this to give our definition of non-empirical parameters. We next give a substantial amount of background material which also serves to define our notation. The main body of the paper is the careful extrapolation, from the results we have for finite Z , to the large- Z limit. We test these extrapolations on cases where we know the answer and show that the results are independent of the details of our procedure. In Sec. IV, we discuss the relevance of our results for the density functional approximations.

We use atomic units throughout, so all energies are in Hartrees and all distances in Bohr radii. All calculations employ spin DFT and are entirely non-relativistic.

We beg the forbearance of the reader, as we close with a simple mathematical illustration of the nature and the usefulness of expansions as $N \rightarrow \infty$, which is the type of expansion we will apply to density functionals. Later, we will tie this particular example to DFT, but for now, consider only the mathematics.

Consider an infinite series with terms,

$$1, 1/4, 1/4, 1/4, 1/4, 1/9, \dots, 1/9, 1/16, \dots, 1/16, 1/25, \dots, \quad (2)$$

i.e., a list of $1/n^2$, but where each value is repeated n^2 times. If f_n is the n th term in this series, suppose we wish to find the partial sum,

$$S_N = \sum_{n=1}^N f_n. \quad (3)$$

This function is plotted in Fig. 1.

Clearly the sum is unbounded as $N \rightarrow \infty$. To expand the series for large N , consider those values at which S is an integer, a condition analogous to filling an atomic shell,

$$S_{M(j)} = j, \quad (4)$$

where

$$M(j) = \sum_{k=1}^j k^2 = j(j+1)(2j+1)/6. \quad (5)$$

Expanding $j(M)$ in inverse powers of $M^{-1/3}$, we find

$$j(M) = (3M)^{1/3} - 1/2 - \dots \quad (6)$$

yielding

$$S_N \rightarrow b_0(N) + b_1(N) + b_2(N) + \dots, \quad (7)$$

where $b_0(N) = (3N)^{1/3}$, $b_1(N) = -1/2$, etc. We then define the sum up to a given order in $N^{1/3}$,

$$B_p(N) = \sum_{k=0}^p b_k(N) \quad (8)$$

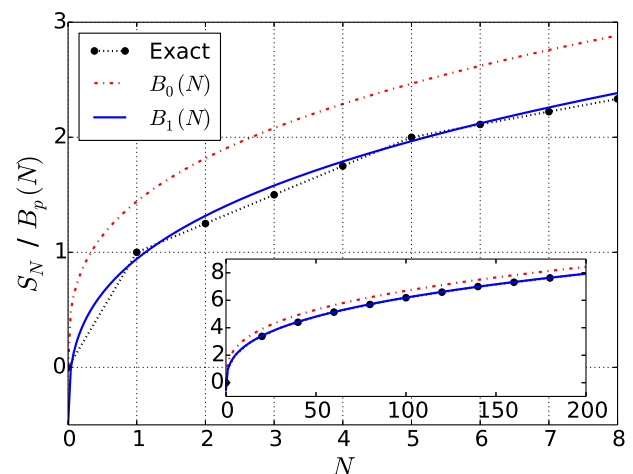


FIG. 1. Partial sum S_N as a function of N and its large- N asymptotic expansion: including just the leading term in $B_0(N)$ and adding the first correction in $B_1(N)$. Inset shows the same plots, but for significantly larger N .

and compare these with the exact curve in Fig. 1. The most important point for now is that including only the first two terms yields a very reasonable approximation to S_N , i.e., the large- N expansion can be used to approximate the series for *any* value of N , all the way down to $N = 1$. Thus, even though we might only care about, e.g., $N < 100$, we can find good approximations by studying the approach to the large- N limit. We will return to this example several times in this article. For now, we also point out several features:

- The leading term, $B_0(N) = (3N)^{1/3}$, is always an overestimate, being 44% too high at $N = 1$, with the error decreasing with increasing N .
- Inclusion of the second term reduces the error to a 6% underestimate for $N = 1$, and now the sign of the error varies. This is almost always a better approximation than $B_0(N)$, except near $N = 0$, where B_0 gives the exact answer, while $B_1 = -1/2$. A physical realization of this expansion and interpretation of B_0 and B_1 is discussed in Sec. II D.
- The first two terms are smooth functions of N , but the exact partial sum S_N has kinks wherever S_N passes through an integer.
- The next term in the series, $b_2(N)$, behaves as $N^{-1/3}$. It is *not* smooth but instead periodic across a shell; thus, it (and all subsequent terms) requires a more careful analysis than that for filled shells.³² We discuss b_2 further in Sec. III F.

II. BACKGROUND AND NOTATION

A. Kohn-Sham DFT

The formal basis of DFT was established first by Hohenberg and Kohn,³³ but we use the more general formulation of Levy here.^{11,12} The ground-state energy of any electronic system can be found from an exact variational principle in the density,

$$E = \min_n \left\{ F[n] + \int d^3r n(\mathbf{r}) v(\mathbf{r}) \right\}, \quad (9)$$

where $v(\mathbf{r})$ is the one-body potential, the minimization is over all normalized non-negative densities with finite kinetic energy,¹² and

$$F[n] = \min_{\Psi \rightarrow n} \langle \Psi | \hat{T} + \hat{V}_{ee} | \Psi \rangle, \quad (10)$$

where \hat{T} is the kinetic energy operator, \hat{V}_{ee} is the electron-electron repulsion, and the minimization is over all normalized antisymmetric wavefunctions.

The original DFT was that of Thomas-Fermi,^{34,35} in which the kinetic energy of the electrons is approximated with a local approximation,

$$T^{\text{TF}}[n] = A_S \int d^3r n^{5/3}(\mathbf{r}), \quad (11)$$

where $A_S = 3(3\pi^2)^{2/3}/10$, and their interaction energy is approximated by the Hartree electrostatic self-energy of the

density,

$$V_{ee}^{\text{TF}}[n] = U[n] = \frac{1}{2} \int d^3r \int d^3r' \frac{n(\mathbf{r})n(\mathbf{r}')}{|\mathbf{r} - \mathbf{r}'|}. \quad (12)$$

Applying such approximations to the total energy, and minimizing to find the density of a system, leads to self-consistent TF theory, which was used for several decades in material calculations.³⁶ The TF equation for an atom is now iconic,^{34,35,37} and was solved numerically in the original papers. Energies are typically accurate to within about 10%, but the theory is too crude for modern chemical and material purposes.³⁶

The variant in use in almost all modern electronic structure calculations is Kohn-Sham (KS) DFT, which posits a fictitious set of non-interacting electrons with the same ground-state density.¹ These electrons satisfy the Pauli principle and obey the KS equations,

$$\left\{ -\frac{1}{2}\nabla^2 + v_S(\mathbf{r}) \right\} \phi_i(\mathbf{r}) = \epsilon_i \phi_i(\mathbf{r}). \quad (13)$$

Writing the energy in terms of these orbitals,

$$E = T_S + U + V + E_{\text{XC}}, \quad (14)$$

where T_S is the kinetic energy of the KS orbitals, U their Hartree energy, and E_{XC} is defined by Eq. (14). For simplicity, we write all equations here in terms of DFT, but in practice, and in our calculations, we use spin-DFT.³⁸

Kohn and Sham also wrote down the most primitive approximation to use in their equations,¹ the local density approximation (LDA) for XC,

$$E_{\text{XC}}^{\text{LDA}} = \int d^3r e_{\text{XC}}^{\text{unif}}(n(\mathbf{r})), \quad (15)$$

where $e_{\text{XC}}^{\text{unif}}(n)$ is the XC energy density of a uniform gas of density n , which is now known very accurately.³⁹⁻⁴¹ This was used for a generation in solid-state physics,^{42,43} but almost always significantly overbinds molecules, so it never became widespread in chemistry. However, most of the properties of molecules in LDA calculations (such as bond lengths and vibrational frequencies) are surprisingly accurate.⁴²

At first, it was thought that LDA might be improved using the gradient expansion,⁴⁴ which includes the leading corrections to the LDA energy for a sufficiently slowly varying gas,

$$E_{\text{XC}}^{\text{GEA}} = E_{\text{XC}}^{\text{LDA}} + \int d^3r g_{\text{XC}}(n) s^2(\mathbf{r}), \quad (16)$$

where $s = |\nabla n|/(2k_F n)$, k_F is the local Fermi wavevector, and $g_{\text{XC}}(n)$ has been derived from many-body theory,^{45,46} at least in the high-density limit. However, in many cases, these corrections worsened LDA results for atoms and molecules. This leads ultimately to the development of modern *generalized* gradient approximations,⁴⁷ which include more general functions of s (but not higher gradients) and led to the widespread use of KS-DFT in chemistry and materials today.⁴⁸ In this language, we can then understand that $T^{\text{TF}} = T_S^{\text{LDA}}$, i.e., the Thomas-Fermi theory approximates the kinetic energy as a local functional of the density for non-interacting electrons.

The standard way to think about XC is in terms of the strength of the Coulomb interaction.³ In DFT, we put a coupling constant λ in front of V_{ee} and imagine varying it, keeping the density fixed. Then, for finite systems,

$$E_{XC}^\lambda = \lambda E_X + E_C^\lambda, \quad (17)$$

where the correlation energy contains only λ^2 and higher powers of λ . Truncation at first order yields exact exchange (EXX), the DFT version of Hartree-Fock⁴⁹ (HF), which yields ground-state energies almost identical to those of HF.⁵⁰

One can relate this λ -dependence to coordinate scaling of the density,⁵¹

$$n_\gamma(\mathbf{r}) = \gamma^3 n(\gamma\mathbf{r}), \quad 0 < \gamma < \infty \quad (18)$$

via

$$E_{XC}^\lambda[n] = \lambda^2 E_{XC}[n_{1/\lambda}]. \quad (19)$$

This can be used to write E_{XC} entirely in terms of a purely potential contribution, the adiabatic connection formula.⁵²⁻⁵⁴ Furthermore, in the absence of degeneracies,

$$T_S[n] = \lim_{\gamma \rightarrow \infty} F[n_\gamma]/\gamma^2 \quad (20)$$

and

$$E_X[n] = \lim_{\gamma \rightarrow \infty} E_{XC}[n_\gamma]/\gamma. \quad (21)$$

B. Lieb-Simon ζ -scaling

We begin with a definition of scaling to large Z . For any system of N non-relativistic electrons with one-body potential $v(\mathbf{r})$, we define a ζ -scaled system following Lieb and Simon,¹³

$$v_\zeta(\mathbf{r}) = \zeta^{4/3} v(\zeta^{1/3}\mathbf{r}), \quad N_\zeta = \zeta N, \quad (22)$$

where ζ is a positive real number. As $\zeta \rightarrow \infty$, this corresponds to simultaneously scaling the coordinates and increasing the particle number. For atoms or ions,

$$v(\mathbf{r}) = -Z/r, \quad v_\zeta(\mathbf{r}) = -\zeta Z/r, \quad (23)$$

i.e., ζ -scaling is simply the same as changing the number of protons and electrons by the same fraction. For molecules and solids, all nuclear separations \mathbf{R} also scale as $\mathbf{R}/\zeta^{1/3}$. The complementary density scaling is

$$n_\zeta(\mathbf{r}) = \zeta^2 n(\zeta^{1/3}\mathbf{r}). \quad (24)$$

This differs from the usual coordinate scaling of Eq. (18) as the particle number also changes. Analogous to that case, the ζ -scaled density is, in general, *not* the ground-state density of the ζ -scaled potential, except within the TF approximation.

C. Lieb-Simon theorem

Lieb and Simon⁵⁵ (LS) rigorously proved that, as $\zeta \rightarrow \infty$,

$$\lim_{\zeta \rightarrow \infty} \frac{E(\zeta) - E^{\text{TF}}(\zeta)}{E(\zeta)} \rightarrow 0 \quad (25)$$

for all non-relativistic Coulombic systems. For example, the percentage error of the energy in a TF calculation for an atom

vanishes for large Z . Moreover, any well-behaved integral over the density of the form¹²

$$I = \int d^3r f(n(\mathbf{r}), \mathbf{r}) \quad (26)$$

will also become relatively exact. Although $n^{\text{TF}}(\mathbf{r})$ has many well-known deficiencies (divergence at the nucleus, non-exponential decay at large distances, missing quantum oscillations), integrals such as I over $n^{\text{TF}}(\mathbf{r})$ have vanishing relative error in this limit.

Without taking too large a leap, we assume that the LS result is also true for non-interacting electrons in any potential,⁵⁶ yielding

$$\frac{T_S(\zeta) - T_S^{\text{TF}}(\zeta)}{T_S(\zeta)} \rightarrow 0, \quad \zeta \rightarrow \infty \quad (27)$$

again, a universal limit of all systems. Thus any approximation that fails to satisfy this limit is unlikely to be a useful starting point for higher accuracy approximations for a large variety of systems.

D. Illustration: Hydrogenic atoms

The simplest useful example of T_S is to consider non-interacting electrons in a hydrogen potential, $-1/r$. Their energies are $-1/2n^2$, where n is the principal quantum number. Via the virial theorem, $T_S = -E$, and accounting for double occupation of the orbitals, in fact,

$$T_S(N) = \frac{1}{2} S_{N/2}, \quad (28)$$

where S_N is the partial sum from the Introduction. Thus our purely mathematical example is in fact a relevant example. The TF density for this problem is simply⁵⁷

$$n^{\text{TF}}(r) = \frac{4Z}{\pi^2 r^3} \left(\frac{r_c}{r} - 1 \right)^{3/2} \Theta(r_c - r), \quad (29)$$

where $r_c = (18/Z)^{1/3}$, and Θ is the Heaviside step function. This situation is similar to the interacting case, in which the TF density is singular at the origin, missing oscillations, and does not decay correctly at large r . Insertion of Eq. (29) into Eq. (11) yields precisely $(3N/2)^{1/3}/2$, the leading term $B_0(N/2)/2$ in the expansion for large N . This is consistent with Eq. (27). Thus, this reasoning says that, for an orbital-free theory to take advantage of the LS result, it should recover both this value and the next correction⁵⁸ ($-1/2$) in the large- Z limit. Of course, this is unlikely to be sufficient to determine a usefully accurate orbital-free DFT. But if the reasoning commonly applied to XC is applied to this problem, i.e., that approximate functionals should build in those conditions that they can satisfy, it is a *necessary* exact condition. No approximate kinetic energy functional known at present produces the correct value for the coefficients of this expansion for all electronic systems.³⁷

E. Exchange-correlation analog

This section addresses a fundamental question about DFT in chemistry and materials science, which is as follows: How can such simple approximations, such as LDA, GGA,

or even hybrids, possibly yield usefully accurate results for such a demanding many-body problem? While their failures for many specific properties and systems are myriad, their successes are legion. How can this be, since everyone knows how demanding and complicated the many-body problem is?

The seeds of the answer are in the Lieb-Simon theorem. As Z grows, local approximations become more accurate for the energy and other integrated quantities (but not pointwise for densities, energy-densities, or potentials). The many-body problem becomes simple in two extremes: $N = 1$ and $N \rightarrow \infty$. All the detailed behaviors of the wavefunctions are averaged away, as quantum oscillations become more and more rapid in space, having less and less effect on system averages.

This then provides a systematic approach to constructing DFT approximations, but one which is entirely different from the traditional approach in terms of many-body theory and expansions in λ , the electron-electron interaction. The Thomas-Fermi approximation becomes relatively exact for large N . Note that we do not claim that our systems of interest have large N , and indeed, a direct large- N expansion of the energy is often not sufficiently accurate. Instead, we apply the large- N DFT approximation self-consistently to the problem at hand. We are using the density functional that is exact at large N , which is much more accurate than simply taking the large- N behavior of our specific system. In terms of our hydrogenic illustration, a GGA for T_S can be constructed that automatically recovers the first two terms in the expansion of the energy, but that is more accurate for small N than the asymptotic expansion alone.³⁷

We now conjecture that the following statement is true for KS-DFT:

$$\lim_{\zeta \rightarrow \infty} \frac{E_{XC}(\zeta) - E_{XC}^{LDA}(\zeta)}{E_{XC}(\zeta)} \rightarrow 0. \quad (30)$$

We call this a conjecture, because the Lieb-Simon theorem for TF theory has been proven rigorously in a mathematical physics sense,⁵⁹ but no such general demonstration yet exists for E_{XC} . However, all evidence suggests that this conjecture is correct. For example, few would doubt that, in a limit in which the number of particles is growing, $E_C/E_X \rightarrow 0$, so that the statement needs only be proven for E_X . This was demonstrated very carefully by Schwinger^{17,18,60-66} for atoms and detailed in the pioneering book of Englert.³² It was later proven rigorously for atoms.²⁰ It can be proven for all systems if the singularity at the nuclei is smoothed,¹⁹ but no general mathematical proof has been given for Coulomb interactions. For our purposes, this is sufficient.

Virtually all modern XC approximations reduce to E_X^{LDA} for uniform densities, which means that they also do so for inhomogeneous systems as $\zeta \rightarrow \infty$. Assuming the conjecture is correct, this makes sense as E_X^{LDA} is then a *universal* limit for all systems, and its relevance has nothing to do with the rapidity of the density variation (which is never slow for realistic finite systems). By studying the exchange energies of noble gas atoms of increasing Z , one can²¹ deduce $E_X^{LDA}[n]$, i.e., it is a simple limit of *all* systems, one in which the many-body problem becomes very difficult (the number of particles is diverging), but in which the density functional for the integrated quantity simplifies enormously.

As $\zeta \rightarrow \infty$, the coupling between electrons becomes weak, just as it happens for $\gamma \rightarrow \infty$, in coordinate scaling. Thus this limit is weakly correlated. But the number of particles is also growing, and the number of pair-interactions is growing even faster. In this limit,⁶⁷

$$V_{ee}[n_\zeta] \rightarrow U[n] + \zeta^{5/3} E_X^{LDA}[n] + \dots \quad (31)$$

If we compare this with the usual coordinate scaling, and speak in terms of the coupling constant, as ζ grows, the effective coupling constant is shrinking. But due to the increased number of interactions, the net effect is as given above. The analog to Eq. (20) using the Lieb-Simon theorem is

$$T_S^{TF}[n] + U[n] = \lim_{\zeta \rightarrow \infty} F[n_\zeta]/\zeta^{7/3} \quad (32)$$

while for XC, the analog to Eq. (21) is

$$E_X^{LDA}[n] = \lim_{\zeta \rightarrow \infty} E_{XC}[n_\zeta]/\zeta^{5/3}. \quad (33)$$

We can then argue that, if standard DFT approximations work reasonably well for weakly correlated systems, it is because the density-dependence of the XC energy, found self-consistently in the KS scheme, is well-approximated by the limiting density functional. Most molecular systems at or near equilibrium bond lengths are weakly correlated, so LDA yields usefully accurate values in this region. While LDA is insufficiently accurate for the energy difference between an equilibrium bond and the dissociated atoms, its error is extremely systematic, and the next correction to the energy in the form of a GGA works reasonably well.

This is entirely analogous to the starting approximation for most many-body treatments. Hartree-Fock becomes relatively exact as the electron-electron repulsion becomes weak. But, in practice, we apply it directly to any many-electron system with the full electron-electron repulsion and find usefully accurate descriptions (although not bond-energetics) from the self-consistent solution of those equations. LDA becomes relatively exact in a different limit, as discussed above. In this sense, LDA is as non-empirical as HF and is substantially more accurate for bond energies.

F. Locality principle

Here we claim that a *locality* principle is at work in DFT: Many of the successes and failures of DFT approximations to XC can be understood in terms of the expansion of the functional around the large- Z , i.e., local limit. The success of LDA for real materials (not slowly varying gases) has nothing to do with the uniform gas per se. It is a universal limit of *all* quantum systems, and that limit is most easily calculated from the uniform gas. The real question is as follows: For real molecules and materials, does LDA dominate, and if so, how large are the corrections? LDA works as well (or as badly) as it does for weakly correlated systems because, for those systems, the density-dependence of the XC energy functional is moderately accurately approximated by its limiting form (i.e., a local one). For such systems, and only such systems, inclusion of the next correction should improve its accuracy. Thus most molecules and many materials at equilibrium are weakly correlated. LDA works reasonably well, and standard GGA's

usually improve energetics substantially. On the other hand, static correlation is a signal that this expansion is failing, and hybrid functionals^{6,68} are a crude attempt to account for this.

We therefore define the beyond-local (BL) XC energy functional as

$$E_{\text{XC}}^{\text{BL}}[n] = E_{\text{XC}}[n] - E_{\text{XC}}^{\text{LDA}}[n] \quad (34)$$

and an obvious question arises: If LDA becomes relatively exact for E_{XC} at large ζ , what approximation for $E_{\text{XC}}^{\text{BL}}[n]$ becomes relatively exact in this limit? This is the natural expansion of which LDA is the leading order, and one can hope that accurate inclusion of the next order will lead to accurate energetics for weakly correlated systems. Presumably, standard GGA's are crude examples of such corrections.

G. A simple example: Exchange

The answers for exchange are simple and well-established.²¹ In this case, for atoms,

$$E_X \rightarrow -A_X Z^{5/3} + B_X Z + \dots \quad (35)$$

The dominant term is exact within LDA, given by

$$E_X^{\text{LDA}}[n] = -\frac{3}{4} \left(\frac{3}{\pi} \right)^{1/3} \int d^3r n^{4/3}(\mathbf{r}). \quad (36)$$

To evaluate this, we write the TF atomic density in dimensionless form,³²

$$n^{\text{TF}}(r) = \frac{Z^2}{4\pi a^3} f(x), \quad (37)$$

where $x = Z^{1/3}r/a$ and $a = (3\pi/4)^{2/3}/2$. Inserting this into Eq. (36) yields³⁷

$$A_X = \left(\frac{9}{2\pi^4} \right)^{1/3} M, \quad M = \int_0^\infty dx x^2 f^{4/3}(x), \quad (38)$$

where M is known numerically to be about 0.615434679.³⁷ Thus $A_X \approx 0.2208274$. The precise value of B_X has not been derived, but estimates for B_X have been extracted numerically by careful extrapolation to the large Z limit of atoms. $B_X^{\text{LDA}} \approx 0$, but $B_X \approx 0.224$, i.e., there is a large beyond-local contribution. The two most commonly used^{4,8} generalized gradient approximations for E_X recover this beyond-local contribution rather accurately, whereas the gradient expansion for the slowly varying gas, when applied as an approximation to atoms, is smaller by about a factor of 2.^{22,67}

H. Non-empirical constants

At this point, we make a small aside about what we mean by the term non-empirical. For simplicity, return to our mathematical example. Suppose we argue (or notice from examples) that the leading term must grow as $N^{1/3}$, and we use some set of tabulated values of S_N to fit the coefficient in $B_0(N)$. If we used just the point $N = 1$, we would get this coefficient quite wrong (1 instead of $3^{1/3} \approx 1.4422$). If we use the first 10 points, we get a more accurate answer. But if, instead, we use tabulated values of S_N to extrapolate the

$N \rightarrow \infty$ value, we get our best estimate of the non-empirical value. For example, knowing S_N for $N = 1-100$, and the form $AN^{1/3} + B$, we can estimate $A = 1.4458$ (versus the exact value of $3^{1/3} = 1.4422$) and $B = 0.525$ (versus $1/2 = 0.5$), by using only the last 50 values.

By contrast, simple fitting (such as a polynomial fit) to a range of finite data, including small N but without accounting for the asymptotic analytic form, will usually produce a numerically more accurate value within the range of the data, but will fail as N grows larger, and might be disastrous when attempting to find the next correction. Note also that it is vital to know the correct form, to guarantee relative exactness as N grows, and to allow investigation of higher-order terms.

Thus, by using tabulated values and the correct form of the expansion, we can estimate a non-empirical coefficient, even though we might not have the ability or energy to derive its value analytically. The larger the values of N that we use, and the more terms in the form, the more accurate our estimate can be. We denote the result as non-empirical, even though it has not been derived analytically, and we do not get the exact analytic value, just a best estimate of it.

III. ATOMIC CORRELATION

A. Data

1. Quantum chemical data

We are almost ready to begin our analysis of the locality of the correlation energy. All our data will come from non-relativistic atomic calculations. Our starting point is the relatively recent publication of total correlation energies of spherical atoms²⁸ up to $Z = 86$ and non-spherical ones⁶⁹ up to $Z = 36$. These add to the well-known benchmark set⁷⁰ up to $Z = 18$, although they are not quite as accurate. It is the existence of these results that make the following analysis possible. Their values appear (with many others) in Tables I and II and are plotted in Fig. 2, in the form of correlation energy per electron.

The behavior of correlation energies across rows of the periodic table, and how it changes as one goes down a column, will play an important role in our analysis, but the data set becomes sparse for large Z . We have therefore performed pure random-phase-approximation (RPA) calculations for all elements up to $Z = 86$, and these results are included in Tables I and II and Fig. 2. We find that these RPA results can be ‘‘asymptotically corrected’’ using a simple formula (68) described later in the manuscript. Using only noble gases as a fitting set, this asymptotically corrected RPA (acRPA) nearly matches QC trends for all atoms for which QC data are available. We thus use the acRPA to ‘‘fill in’’ gaps in the reference data set.

2. RPA calculations

The adiabatic connection formula⁵²⁻⁵⁴ combined with the fluctuation-dissipation theorem (ACFD) and the RPA is fast becoming a *de facto* standard⁷¹⁻⁷³ for calculations of nearly quantum chemical accuracy energy differences. Unfortunately,

TABLE I. Negative of atomic correlation energies per electron in Ha. “Bench” is benchmark data from Refs. 28, 69, and 70 and “acRPA” is asymptotically corrected RPA [RPA + Eq. (68)]. Listed errors are the deviation from the “bench” value (where available) or “acRPA” otherwise. Numerical errors on “bench” are estimated to be within 2.2% for $Z \leq 54$ and 3.5% for larger atoms^{28,69} while errors on “acRPA” could be up to 5.5% (including numerical errors and differences between EXX and HF energies). Errors on LDA and PBE are estimated to be around 1 mhartree/electron.

N	Bench	RPA	Err	acRPA	Err	LDA	PBE	Err
1	0.0	20.9	20.9	-5.0	-5.0	21.7	5.7	5.7
2	21.0	42.0	21.0	18.6	-2.4	55.5	20.5	-0.5
3	15.1	37.8	22.7	15.4	0.3	50.1	17.0	1.9
4	23.6	45.6	22.0	23.6	0.0	55.9	21.4	-2.2
5	25.0	45.5	20.5	23.8	-1.2	57.9	23.1	-1.9
6	26.1	46.6	20.6	25.1	-0.9	59.5	24.5	-1.6
7	26.9	48.7	21.8	27.4	0.5	60.8	25.5	-1.4
8	32.2	51.9	19.7	30.7	-1.6	66.7	29.5	-2.7
9	36.1	55.8	19.7	34.6	-1.5	70.9	32.5	-3.6
10	39.1	60.1	21.0	39.0	-0.1	74.0	34.7	-4.4
11	36.0	57.2	21.1	36.2	0.1	72.7	33.5	-2.5
12	36.6	57.5	20.9	36.5	-0.1	73.9	34.1	-2.5
13	36.2	56.6	20.4	35.7	-0.5	74.0	34.3	-1.9
14	36.1	56.5	20.4	35.7	-0.5	74.0	34.6	-1.5
15	36.1	57.1	21.1	36.3	0.2	74.2	35.0	-1.1
16	37.9	58.2	20.3	37.4	-0.5	76.3	36.6	-1.3
17	39.3	59.7	20.4	38.9	-0.4	77.8	38.0	-1.3
18	40.3	61.5	21.2	40.8	0.4	79.1	39.1	-1.2
19	40.2	61.1	20.9	40.4	0.2	78.4	38.5	-1.7
20	41.3	62.1	20.8	41.4	0.1	78.8	38.7	-2.6
21	42.2	62.7	20.5	42.0	-0.2	79.6	39.3	-2.8
22	42.9	63.4	20.5	42.7	-0.2	80.3	40.0	-2.9
23	43.7	64.3	20.6	43.7	-0.0	80.1
24	44.6	65.4	20.9	44.8	0.2	80.7	41.0	-3.6
25	45.2	66.7	21.5	46.0	0.8	82.1	41.7	-3.5
26	47.5	68.2	20.7	47.6	0.1	83.7	42.9	-4.6
27	49.1	69.8	20.6	49.2	0.0	85.5	44.5	-4.7
28	50.9	71.5	20.6	50.9	0.0	86.7	45.4	-5.5
29	54.6	73.3	18.7	52.7	-1.9	87.7	46.2	-8.4
30	54.0	75.2	21.2	54.7	0.7	88.4	46.7	-7.3
31	52.7	73.5	20.7	52.9	0.2	88.6	46.8	-5.9
32	51.8	72.4	20.6	51.9	0.1	88.6	47.0	-4.7
33	51.0	71.8	20.8	51.3	0.2	88.7	47.2	-3.8
34	51.2	71.5	20.4	51.0	-0.2	89.6	47.9	-3.3
35	51.3	71.6	20.3	51.1	-0.2	90.3	48.5	-2.8
36	51.4	71.9	20.5	51.4	0.0	90.8	49.0	-2.4

it is well known that RPA gives poor estimates of *absolute* correlation energies. As we will show later, this erroneous contribution can, at least in the atomic systems considered here, be cancelled by a simple fit, Eq. (68), depending on the number of electrons only. This thus renders corrected RPA suitable for accurate correlation energy calculations of atoms, on a par with the most accurate quantum chemical benchmarks.

RPA energies are calculated using the ACFD correlation energy formula

$$E_C = \int_0^1 d\lambda \int d^3r d^3r' \frac{n_{2C}^\lambda(\mathbf{r}, \mathbf{r}')}{2|\mathbf{r} - \mathbf{r}'|}. \quad (39)$$

TABLE II. Same as Table I, but larger Z .

N	Bench	RPA	Err	acRPA	Err	LDA	PBE	Err
37	...	71.2	20.5	50.7	...	90.4	48.6	-2.1
38	51.0	71.4	20.3	50.9	-0.2	90.6	48.7	-2.4
39	...	71.5	20.5	51.0	...	90.8	48.9	-2.2
40	...	71.6	20.5	51.1	...	91.0	49.1	-2.0
41	...	71.8	20.5	51.3	...	90.7	49.3	-2.0
42	...	72.1	20.5	51.6	...	90.8
43	...	72.5	20.5	52.1	...	91.6	49.9	-2.2
44	...	73.0	20.4	52.6	...	92.6	50.9	-1.6
45	...	73.6	20.4	53.2	...	93.3	51.5	-1.6
46	55.3	74.3	19.0	53.8	-1.4	94.4	52.5	-2.8
47	...	75.0	20.4	54.5	...	94.5	52.6	-1.9
48	55.2	75.7	20.5	55.3	0.1	94.8	52.8	-2.4
49	...	75.2	20.4	54.8	...	94.8	52.8	-2.0
50	...	75.0	20.4	54.6	...	94.8	52.9	-1.6
51	...	75.0	20.4	54.5	...	94.8	53.0	-1.6
52	...	75.1	20.4	54.7	...	95.3	53.4	-1.3
53	...	75.4	20.4	55.0	...	95.6	53.7	-1.3
54	55.6	75.9	20.3	55.5	-0.1	95.9	54.0	-1.5
55	...	76.2	20.4	55.8	...	95.6	53.7	-2.1
56	55.8	76.5	20.7	56.1	0.3	95.7	53.7	-2.1
57	...	77.1	20.4	56.7	...	95.8	53.9	-2.8
58	...	77.9	20.4	57.5	...	96.4	54.4	-3.1
59	...	78.7	20.4	58.3	...	96.7	54.7	-3.5
60	...	79.4	20.4	59.0	...	97.1	55.0	-4.0
61	...	80.1	20.4	59.7	...	97.4	55.3	-4.4
62	...	80.9	20.4	60.5	...	97.7	55.6	-4.9
63	...	81.7	20.4	61.3	...	98.0	55.9	-5.4
64	...	82.5	20.4	62.1	...	98.1	56.0	-6.1
65	...	83.4	20.4	63.0	...	99.2	56.9	-6.2
66	...	84.3	20.4	64.0	...	99.7	57.3	-6.6
67	...	85.3	20.4	64.9	...	100.2	57.8	-7.2
68	...	86.3	20.4	65.9
69	...	87.3	20.3	67.0	...	101.1	58.6	-8.4
70	67.0	88.4	21.4	68.1	1.0	101.6	59.0	-8.1
71	...	87.3	20.3	67.0	...	101.7	59.1	-7.9
72	...	86.4	20.3	66.1	...	101.9	59.2	-6.8
73	...	85.7	20.3	65.3	...	102.0	59.4	-5.9
74	...	85.2	20.3	64.9	...	102.1	59.5	-5.3
75	...	84.9	20.3	64.5	...	102.2	59.7	-4.9
76	...	84.7	20.3	64.4	...	102.7	60.0	-4.3
77	...	84.6	20.3	64.3	...	103.1	60.4	-3.9
78	...	84.6	20.3	64.3	...	103.6	60.9	-3.4
79	...	84.7	20.3	64.4	...	103.9	61.2	-3.2
80	64.7	84.8	20.1	64.5	-0.2	104.0	61.3	-3.4
81	...	84.3	20.3	64.0	...	104.0	61.3	-2.7
82	...	84.0	20.3	63.6	...	104.0	61.3	-2.3
83	...	83.8	20.3	63.4	...	103.9	61.3	-2.1
84	...	83.7	20.3	63.4	...	104.2	61.5	-1.8
85	...	83.7	20.3	63.4	...	104.4	61.7	-1.7
86	64.2	83.9	19.6	63.6	-0.7	104.6	61.9	-2.3

Here the pair-density n_{2C}^λ is found from the fluctuation dissipation theorem via

$$n_{2C}^\lambda(\mathbf{r}, \mathbf{r}') = \int_0^\infty \frac{d\omega}{\pi} [\chi^\lambda(\mathbf{r}, \mathbf{r}'; i\omega) - \chi^0(\mathbf{r}, \mathbf{r}'; i\omega)], \quad (40)$$

$$\chi^0 = 2\mathfrak{K} \sum_i f_i \phi_i(\mathbf{r}) \phi_i(\mathbf{r}') G(\mathbf{r}, \mathbf{r}'; \epsilon_i - i\omega), \quad (41)$$

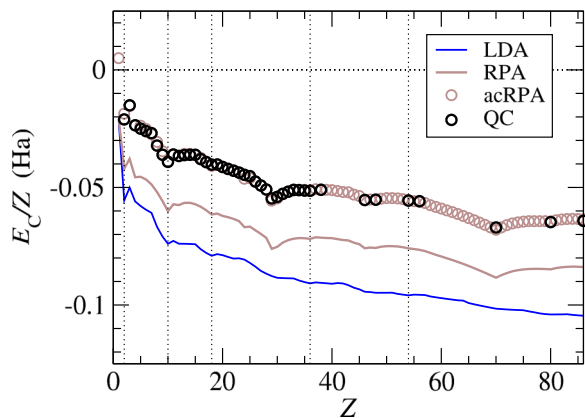


FIG. 2. Correlation energy per electron versus Z for accurate quantum chemistry (QC) calculations (black circles), the RPA (brown solid line), corrected RPA data (brown circles), and the local density approximation (LDA) of DFT. Circle size matches the maximum reported error of QC data.

$$\chi^\lambda = \chi^0 + \lambda \chi^0 \star \frac{1}{|\mathbf{r} - \mathbf{r}'|} \star \chi^\lambda, \quad (42)$$

where stars indicate spatial convolutions. The non-interacting response χ_0 takes as input the Kohn-Sham orbitals ϕ_i and energies ϵ_i obeying $\{-\frac{1}{2}\nabla^2 + v_S - \epsilon_i\}\phi_i = 0$, and KS Greens functions $G(\mathbf{r}, \mathbf{r}'; \epsilon_i - \omega)$ obeying $\{-\frac{1}{2}\nabla^2 + v_S - \epsilon_i + i\omega\}G(\mathbf{r}, \mathbf{r}'; \epsilon_i - i\omega) = -\delta(\mathbf{r} - \mathbf{r}')$. We work from spherical and spin symmetric groundstates which make all calculations essentially one-dimensional. All equations can thus be carried out using a large radial grid which helps to reduce numerical errors in (39). Errors are estimated to be well under 1.1 mhartree/electron. We use the same algorithms and code as previous work.^{74,75}

Equation (39) is an indirect orbital function which formally maps a Kohn-Sham potential v_S and orbital occupation factors f_i to a correlation energy. We must thus start from a reasonably accurate potential if we are to expect accurate energies. For this work, we perform RPA calculations using strictly spherical Kohn-Sham potentials calculated using LEXX⁷⁴ theory extended to d and f shells. LEXX yields a Hartree and exchange energy functional of the same form as HF theory, but in which all orbitals are systematically calculated in a multiplicative spherically symmetric potential. Its associated correlation energy is thus slightly larger in magnitude. For most elements, the occupation factors are assigned according to Hund's rules, in accordance with the theoretical and experimental evidence. For the transition metals, we use the lowest energy orbital filling (in exact exchange theory) of the s and d shells (e.g., $4s^1 3d^{10}$ for Cu and $5s^1 4d^4$ for Nb), which allow ready comparison with the results of McCarthy and Thakkar.⁶⁹ For the atoms in row 6, we simply fill the orbitals according to Hund's rules to avoid the issues of (near-)degeneracy.

Ideally the orbitals would be calculated on the exact Kohn-Sham potential $v_S(\mathbf{r})$, but this is available for only a very limited number of atoms, forcing us to use an appropriate approximation to the potential. The LEXX potential was chosen due to its good asymptotic form and inclusion of static correlation in open shell systems. To ensure that our RPA energies are appropriate, we performed some additional

tests to study dependence on the potential. First, for C and F we evaluated RPA energies using both the exact⁷⁶ potential and the LEXX potential and found the difference to be less than 0.3 mhartree/electron. We also compared energies calculated using the PBE potential and LEXX potential across many species and found a maximum difference of 1.0 mhartree/electron, a likely worst case scenario. We thus assume our total error (numerical and error from the potential) to be under 1.5 mhartree/electron or 3%, whichever is the larger. This gives us, through RPA and the corrections discussed later, accurate benchmarks for all non-relativistic atoms with up to 86 electrons.

3. DFT calculations

At the opposite end of the scale, one can perform atomic DFT calculations of correlation energies rather simply and go to much larger Z than with correlated wavefunction treatments. For the purposes of our study, we include all Z up to 86 and use both LDA and PBE results. We use the PW92 parametrization of the uniform gas,⁴¹ the relevance of which will be discussed below. We include PBE because, as shown below, its form mimics that of the exact functional in the large Z limit, so that the large- Z behavior can be most easily extracted by comparison with that approximation.

4. Results

Tables I and II list all our results. In Fig. 2, we plot correlation energies per electron as a function of Z , as well as the RPA and LDA results. The shapes are well-known and unsurprising. The RPA significantly overcorrelates the atoms, and the LDA is even worse. Many quantum chemists question the value of LDA for such calculations, as the relevance of the uniform gas for such systems is far from obvious. Indeed, from this figure alone, it is unclear that the QC correlation energy per electron is diverging logarithmically — the limiting behavior of Eq. (1) derived from the uniform gas. One could reasonably argue that it is approaching a constant for sufficiently large Z . We demonstrate below that the latter is definitely *not* the case.

Note that the difference between HF energies^{69,77} and Kohn-Sham exact-exchange (EXX) energies (as computed in our work) is smaller than other errors, so we ignore this difference here.

B. Theory

We now test the locality conjecture for correlation and use it to extract trends in Fig. 2 and Table I. The conjecture implies that

$$E_C[n_\zeta] \rightarrow E_C^{\text{LDA}}[n_\zeta^{\text{TF}}], \quad \zeta \rightarrow \infty. \quad (43)$$

Thus we begin with the local density approximation, which uses the correlation energy of a uniform gas,

$$E_C^{\text{LDA}}[n] = \int d^3r n(\mathbf{r}) \epsilon_C^{\text{unif}}(n(\mathbf{r})), \quad (44)$$

where $\epsilon_C^{\text{unif}}(n)$ is the correlation energy per electron. This is a non-trivial function of the density that is now well-known from many-body theory and quantum Monte Carlo simulations of the uniform gas.³⁹ There are several almost identical parametrizations^{40,41} in common use. Our interest is the large- ζ limit, which is dominated by high densities. In a landmark of electronic structure theory, Gell-Mann and Brueckner⁷⁸ applied the random phase approximation (RPA) to the uniform gas to find

$$\epsilon_C^{\text{unif}} = c_0 \ln r_s - c_1 + \dots, \quad r_s \rightarrow 0, \quad (45)$$

where $r_s = (3/(4\pi n))^{1/3}$ is the Wigner-Seitz radius of density n , $c_0 = 0.031091$, and $c_1^{\text{RPA}} = 0.07082$. In fact, Eq. (45) yields the exact high-density limit if $c_1 = 0.04664$, the correction from RPA being due to the second-order exchange.⁷⁹ But, as is clear in Fig. 2, LDA¹ greatly overestimates the magnitude of the correlation energy of atoms (factor of 2 or more). For atoms with large Z , insert $n^{\text{TF}}(\mathbf{r})$ into Eq. (44) to find

$$E_C^{\text{LDA}} = -A_C Z \ln Z + B_C^{\text{LDA}} Z + \dots, \quad (46)$$

where $A_C = 2c_0/3 = 0.02073$. B_C^{LDA} is found by considering the contributions linear in Z generated by replacing Eq. (37) in the high-density limit of $E_C^{\text{LDA}}[n]$. As a result,

$$B_C^{\text{LDA}} = \frac{c_0}{3} [\ln(3a^3) - I_2] - c_1, \quad (47)$$

where

$$I_2 = \int_0^\infty dx f(x) \ln[f(x)] \quad (48)$$

and is known numerically to be about -3.331462 .³⁷ This yields

$$B_C^{\text{LDA}} = -0.00451, \quad (49)$$

as reported in Ref. 67.

The locality conjecture, applied to correlation alone, implies that the leading term of Eq. (46) is exact. In fact, this has been proven for atoms relatively recently,²⁹ which shows definitively that the curves in Fig. 2 do not saturate. It also suggests that we define

$$e_{\text{AC}}(Z) = E_C/Z + A_C \ln Z \quad (50)$$

as the asymptotically corrected correlation energy per electron. This is plotted in Fig. 3. Now the curves do appear to saturate, although the oscillations across open shells make accurate extrapolation of the large- Z limit very difficult. For any such curve, we define

$$B_C = \lim_{Z \rightarrow \infty} e_{\text{AC}}(Z), \quad (51)$$

and try to estimate this value as accurately as possible. This will be the subject of Sec. III D.

But to get a quick idea, using techniques that have worked for exchange,^{21,37} we largely eliminate the effect of shell structure by taking only noble gas atoms and plot as a function of $1/n_{\text{HOMO}}$, the principal quantum number of the highest occupied shell, as in Fig. 4. Clearly, the RPA and LDA values of B_C are quite different from the reference QC value. (The PBE correlation functional⁸ is included, as its asymptotic

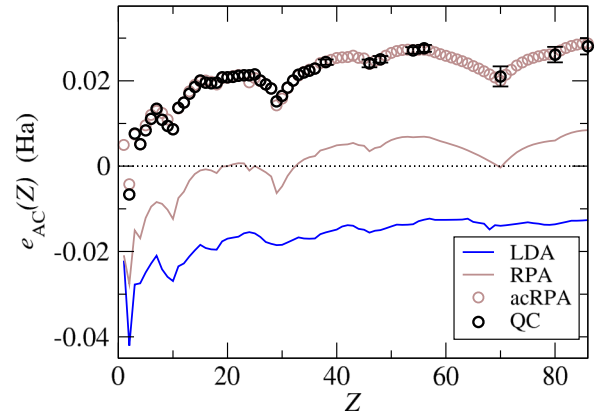


FIG. 3. Asymptotically corrected correlation energy per electron [Eq. (50)] versus Z for accurate quantum chemistry (QC) calculations (black circles), the RPA (brown solid line), corrected RPA data (brown circles), and LDA.

behavior is almost perfectly parallel to the benchmark data, and we use this in Sec. III D to improve our extrapolation.) Repeating the procedure for alkali earths shows that almost identical results occur, as shown in Fig. 5. Fitting noble gas data to the form

$$e_{\text{AC}}^{\text{nob}}(n_{\text{HOMO}}) = B_C^{\text{nob}} - C_C^{\text{nob}}/n_{\text{HOMO}}, \quad (52)$$

we find $B_C^{\text{nob}} = 0.0371$ and $C_C^{\text{nob}} = -0.0536$. Repeating the fit for the alkali earths, we find $B_C^{\text{AE}} = 0.0378$ and $C_C^{\text{AE}} = -0.0644$, reflecting a consistency in the value of B_C extracted from either series.

Finally we can convert our numerical extrapolation versus n_{HOMO} into a smooth function $e_{\text{AC}}^{\text{nob}}(Z)$ in order to explore trends across the entire periodic table. To do so, first, notice that the data oscillate slightly around each fit, with every other point being above or below. This reflects the double-step in the periodic table between the appearance of new rows. To account for this, while still analyzing atoms down a given column, we define

$$\tilde{n}^{\text{nob}}(Z) = (6Z + 8)^{1/3} - 2, \quad (53)$$

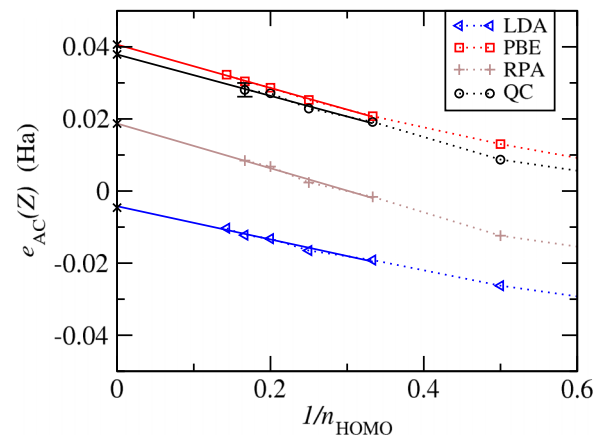


FIG. 4. Asymptotically corrected correlation energy per electron as a function of inverse highest occupied shell for noble gases, for accurate quantum chemistry data (QC), and within RPA, LDA, and PBE. For QC, the error for Rn is shown, others are smaller than data point size.

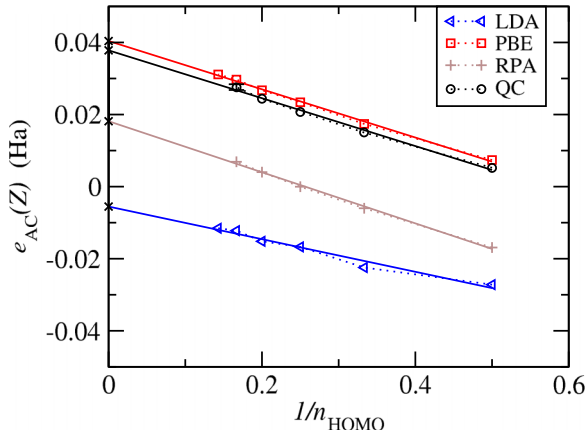


FIG. 5. Same as Fig. 4, but for alkali earths.

which smoothly interpolates n_{HOMO} between even and odd noble gas atoms and is asymptotically correct as $Z \rightarrow \infty$.⁸⁰ We can now write

$$e_{\text{AC}}^{\text{nob}}(Z) = B_{\text{C}}^{\text{nob}} - C_{\text{C}}^{\text{nob}}/\tilde{n}^{\text{nob}}(Z), \quad (54)$$

an estimate of e_{AC} for all Z . To repeat the process for the alkali earths, we use $\tilde{n}^{\text{nob}}(Z-2) + 1$ instead of $\tilde{n}^{\text{nob}}(Z)$ in Eq. (54), and the AE coefficients B_{C}^{AE} and C_{C}^{AE} . The two asymptotic energies converge rapidly onto each other for large- Z , as shown in Fig. 8.

Having identified that B_{C} appears to approach a finite value, in Sec. III D, we make a variety of constructions in order to estimate its value as accurately and reliably as possible from the available data. We also use some of the same techniques to fill in large- Z non-spherical atomic correlation energies in Tables I and II.

C. Testing extrapolation methods on LDA

As an obvious test of our numerical extrapolation methods, we consider self-consistent LDA calculations for neutral atoms. Because such calculations are of irrelevant computational cost, we enlarge the data set up to $Z = 460$. This is the 12th row of the non-relativistic periodic table, assuming Madelung's rule continues indefinitely. Note that any calculations beyond $Z = 100$ are simply a mathematical device to reduce the range of Z over which we extrapolate.

As we go to larger Z , we find even/odd oscillations becoming less problematic; they can be largely eliminated by averaging over the noble gas and the alkali earth atom in each row. These are both spherical (and so appear in our original QC data set) and not spin polarized. In Fig. 6, we plot the averaged results of self-consistent LDA calculations (squares connected by dotted line), the linear extrapolation of these to the asymptotic limit (solid line), and mark the analytical form of this limit from Eq. (47). The LDA energy evaluated on the TF density for each value of Z (dashed line) is also shown.

One can see that the naïve linear trend of e_{AC} with $1/n_{\text{HOMO}}$ must eventually fail for $1/n_{\text{HOMO}} < 0.1$. This occurs even when the TF density is used, due to the logarithmic terms in the high-density expansion of $\epsilon_{\text{C}}^{\text{unif}}$. The difference between

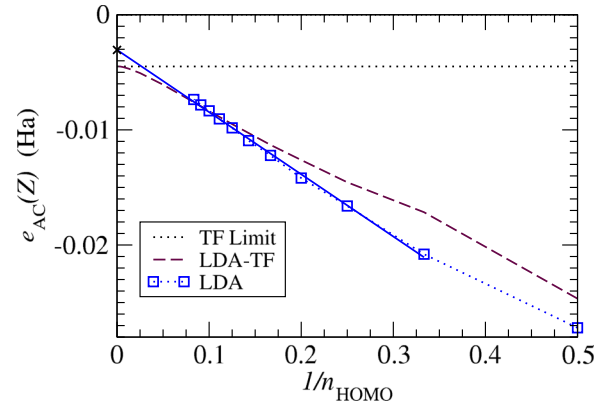


FIG. 6. Asymptotically corrected correlation energy per electron versus $1/n_{\text{HOMO}}$. Squares show self-consistent LDA energies for the alkali earth Be ($n_{\text{HOMO}} = 2$) and also the average of noble gas and alkali earth for $n_{\text{HOMO}} \geq 3$. Solid line is linear fit extrapolating $n_{\text{HOMO}} \rightarrow \infty$, and dashed shows LDA evaluated with asymptotic Thomas-Fermi density. The horizontal line is at the analytic value of $B_{\text{C}}^{\text{LDA}}$.

the self-consistent and TF curves also appears to be non-linear in this region. To understand this, we expand the uniform gas energy in the high-density limit to the next two orders beyond Eq. (45),

$$\epsilon_{\text{C}}^{\text{LDA}} = c_0 \ln r_s - c_1 + c_2 r_s \ln r_s - c_3 r_s, \quad r_s \rightarrow 0, \quad (55)$$

where $c_2 = 0.0066$ and $c_3 = 0.0104$ are known from perturbation theory.⁴¹ Inserting the TF density yields

$$e_{\text{AC}}^{\text{LDA}}[n^{\text{TF}}](Z) \rightarrow B_{\text{C}}^{\text{LDA}} + (\tilde{C}_{\text{C}} \ln Z + \tilde{D}_{\text{C}})/Z^{2/3}, \quad (56)$$

where

$$\tilde{C}_{\text{C}} = -\frac{2}{3}c_2\langle r_s \rangle = -0.051 \quad (57)$$

and

$$\tilde{D}_{\text{C}} = [c_3\langle r_s \rangle + c_2\langle r_s \ln(r_s) \rangle] = 0.207. \quad (58)$$

In these equations, $r_s = a(3/f(x))^{1/3}$ is the local Wigner-Seitz radius of the TF density for $Z = 1$, and

$$\langle g \rangle = \int_{-\infty}^{\infty} dx x^2 f(x) g(x). \quad (59)$$

The important feature is that this expansion is ill-behaved. The culprit is the nature of the average over TF density [Eq. (59)], as $x^2 f(x)[r_s(x)]^n$ decays only as x^{2n-4} as $x \rightarrow \infty$. As a consequence, these next two terms, of order $n = 1$, have much larger coefficients than the leading, order $n = 0$ terms of Eq. (45), and the following two terms diverge on the TF density. This poor behavior is inherited from the uniform gas and shows how unsuitable all but the leading terms of the LDA are for approximating the correlation energy of atoms. Furthermore, it causes the structure we see in the figure as $Z \rightarrow \infty$. Thus, the LDA curve is especially difficult to extrapolate accurately. Nonetheless, performing a naïve application of the linear extrapolation for $n_{\text{HOMO}} \geq 3$ yields -3.0 mhartree, an underestimate of 1.5 mhartree from the analytic value. Thus we expect no larger error from our extrapolation process.

D. Accurate estimate of B_C

Finally, we perform the extrapolation that produces our best estimate for B_C . To achieve the maximum accuracy, we compare the accurate QC data with PBE results.⁸ The primary reason is that the PBE functional was constructed to yield an accurate finite result in this limit, by correcting the LDA energy. Our use here is simply that we can extrapolate the difference between QC and PBE, while extracting the PBE result analytically. The parallel trends in n_{HOMO} for the PBE and QC in Figs. 4 and 5 imply that their difference tends to a constant. Thus the resulting fit ought to be almost exclusively a measure of B_C , with minimum influence from the details of the fit.

The PBE beyond-local correlation energy for spin-unpolarized densities is⁸

$$E_C^{\text{BL,PBE}}[n] = \int d^3r n(\mathbf{r}) h_C^{\text{PBE}}(r_S(\mathbf{r}), t(\mathbf{r})), \quad (60)$$

where $t = |\nabla n|/(2k_s n)$ is the dimensionless gradient for correlation, $k_s = 2(3n/\pi)^{1/6}$ is the TF screening length, and

$$h_C^{\text{PBE}}(r_S, t) = c_0 \ln \left(1 + \frac{\beta}{c_0} t^2 f_C(\tilde{A}r^2) \right), \quad (61)$$

where

$$f_C(y) = (1 + y)/(1 + y + y^2), \quad (62)$$

$$\beta \tilde{A}^{-1} = c_0 [\exp(-\epsilon_C^{\text{unif}}/c_0) - 1], \quad (63)$$

and $\beta = 0.066725$. This peculiar combination of functions results from requiring it to reduce to LDA for uniform densities, yield a finite value in the high-density limit of finite systems, and, when combined with PBE exchange, recover the LDA linear response for a uniform electron gas.⁸ It is the first two conditions which ensure that it yields a finite value for B_C that differs from LDA.

B_C^{PBE} is found by considering the contributions linear in Z generated by replacing Eq. (37) in the high-density large- Z limit, where $\tilde{A} \rightarrow 1/r_S$, $y \rightarrow 0$, and $f_C \rightarrow 1$. As a result,

$$\Delta B_C^{\text{PBE}} = c_0 I_3(\beta/c_0), \quad (64)$$

where

$$I_3(u) = \int_0^\infty dx x^2 f(x) \ln \left(1 + \frac{u}{\sqrt{6}} \frac{df/dx}{f^{7/6}(x)} \right) \quad (65)$$

is a well-defined integral over the TF density.³⁷ For $u = \beta/c_0 = 2.146119$, we find $I_3 = 1.411164$, yielding

$$B_C^{\text{PBE}} = 0.03936 \quad (66)$$

in agreement with Ref. 67.

In Fig. 7, we plot the energy difference in mhartree between QC and PBE per electron. Because the difference is so small, on this scale, the differences between noble gases and alkali earths are very visible, especially for odd rows. But their mean is seen to converge nicely. A fit yields

$$(E_C - E_C^{\text{PBE}})/Z = -0.00215(34) + 0.0000(11)/n_{\text{HOMO}}. \quad (67)$$

Combining the analytic result of Eq. (66) with this one, we conclude that the asymptotic value of B_C is 37.2 mhartree.

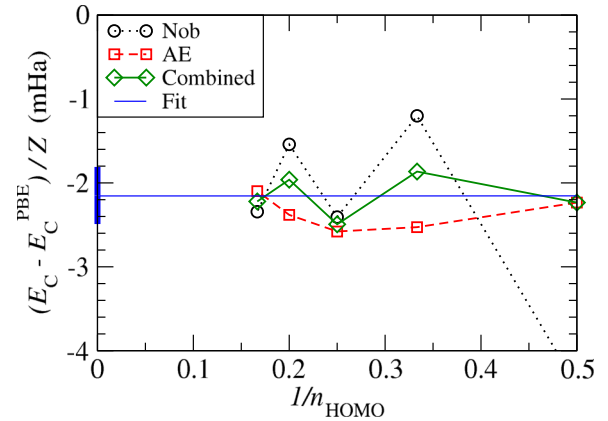


FIG. 7. Difference between the correlation energy-per-electron of QC data and the PBE for noble gas (Nob) and alkali earth (AE) atoms, plotted versus $1/n_{\text{HOMO}}$, along with the combined averages for $n_{\text{HOMO}}=3$ through $n_{\text{HOMO}}=6$. Linear fit [Eq. (67)] in blue, with error bar in the $1/n_{\text{HOMO}}=0$ asymptote shown as solid thick bar. Units in mhartree.

Table III compares the different estimates, showing their consistency, and suggesting the extrapolation error is no more than 1.5 mhartree.

E. Corrections to RPA

There is considerable current interest in using RPA and beyond-RPA methods for quantum chemistry.⁸¹ While many good features are known, a major drawback to pure RPA calculations for thermochemistry is the inaccuracy of RPA atomic energies and its impact on atomization energies.

Unfortunately, the quantum chemical data become sparse for large Z , being limited to spherical atoms. However, our RPA calculations are less limited, and their error relative to the quantum chemical data set is relatively simple. We fit the differences between the RPA correlation energies and the QC ones for noble-gas atoms using

$$\Delta E_C^{\text{RPA}}/Z = 0.0199 + 0.00246/\tilde{n}^{\text{nob}}(Z), \quad (68)$$

where $\tilde{n}^{\text{nob}}(Z)$ is given by Eq. (53). We denote by acRPA the RPA energies with the correction of Eq. (68) added to them. The results are presented in Tables I and II.

In Fig. 8, we plot both the accurate correlation energies and the acRPA values, and the residual error. Clearly, the fit is extremely accurate and errors become negligible for large enough Z . Finally, we note that the constant contribution to the fit, 19.9 mhartree, is close to (but different from) the error

TABLE III. Values for B_C in different approximations via numerical extrapolation and analytically. Reported errors, in parentheses, are statistical errors in the linear regression used to make the extrapolation. Errors in extrapolation can also be judged from the DFT cases where analytic results are known. The QC values are consistent with the best estimate of 37.2 mhartree from Fig. 7.

	AE	Noble	Analytic
LDA	-5.9(16)	-5.0(1.1)	-4.51
PBE	40.2(7)	40.2(5)	39.3
RPA	18.1(7)	18.7(1.4)	15.2
QC	37.8(9)	37.1(1.6)	N/A

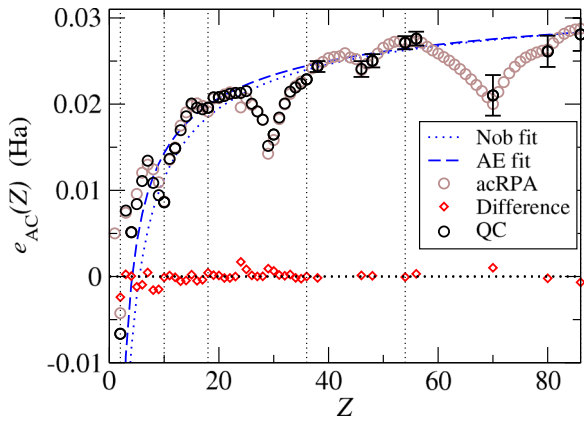


FIG. 8. Asymptotic correction of RPA data: black points are QC data, brown are RPA data corrected via Eq. (68), and red, their difference. Also shown as dashed and dotted lines, smooth asymptotic curves $e_{AC}^{AE}(Z)$ and $e_{AC}^{nob}(Z)$ defined through Eq. (54) and the text following.

the RPA makes for the correlation energy per electron in the high density limit of the uniform gas, 24.2 mhartree, as discussed in Section III B. We can understand one contribution to this difference by considering the PBE for RPA correlation energies developed by Kurth and Perdew.⁸² The expression of the corresponding enhancement factors is reported in Eq. (27) of Ref. 83, from which we readily obtain

$$B_C^{\text{PBE-RPA}} = 0.01518, \quad (69)$$

the difference with PBE being again due to RPA correlation energy of the uniform gas. Since the PBE construction uses the value of the gradient expansion coefficient β from the high-density limit in the RPA approximation, the *gradient* contributions to B_C^{PBE} and B_C^{RPA} are the same. Assuming this procedure is highly accurate for approximating RPA, the remaining difference is only 3 mhartree—well within the numerical error bars for RPA correlation energies, estimated to be up to 4.6 mhartree (3% of 84 mhartree) for $Z = 86$.⁸⁴

Note that this correction formula concerns the relation between an approximation to the many-electron problem and the exact result and is entirely independent of any density functional analysis. Its value is that we can create an enhanced data-set of the QC data, plus RPA-corrected estimates for the larger open-shell atoms. We use acRPA for benchmark values wherever QC values are unavailable, i.e., the non-spherical atoms of Table II. Our simple atomic correction, Eq. (68), is remarkably accurate, as shown in Tables I and II, with few errors greater than 1 mhartree. A scheme which reproduces this correction, but also works well for molecules at equilibrium bond lengths, would overcome the limitations of pure RPA. We suggest testing existing schemes for their behavior in the large- Z limit, characterizing them by the value of B_C .

F. Deviations from smooth functions of Z

To motivate this final section, we return to the didactic example from the Introduction. In Fig. 9, we show (blue dotted line) the error in the asymptotic curve $B_1(N)$ derived in that section and plotted in Fig. 1. Subtracting the mean value of $b_2(N)$ across a shell, $[-12(3N)^{1/3}]^{-1}$, yields the error on B_1^*

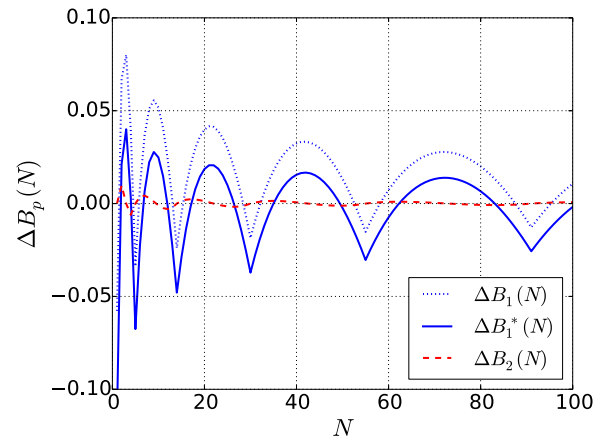


FIG. 9. Errors $\Delta B_p(N) = B_p(N) - S_N$ ($N \geq 1$) in partial sums $B_p(N)$ [Eq. (8)] to different orders for the mathematical series from the Introduction. The blue solid curve (B_1^*) has the mean of $b_2(N)$ subtracted, to emphasize the shell structure.

shown as a blue solid line. This error is not a smooth function of N but has cusps at shell boundaries, is periodic in ν , the fraction of the shell that is filled, and only slowly decaying with shell number. Careful analysis³² yields

$$b_2(N) = \frac{1 - 12\nu(1 - \nu)}{12(3N)^{1/3}}, \quad (70)$$

and addition of this term to form $B_2(N)$ yields the error shown as red dashes. The errors between shells are reduced by an order of magnitude relative to $B_1(N)$, and the error for $N = 1$ is a mere 3×10^{-5} , i.e., 30 μH . Thus it behooves us to look at the structure of such terms.

Of course, exchange and correlation of real atoms is much more complicated, and we do not have access to the exact asymptotic expansion for these quantities. But as our example shows, we may numerically illustrate the nature of the underlying higher-order asymptotic corrections simply by showing the deviation of our data from smooth behavior. To do so, we first obtain smooth curves from our analysis of QC data from single columns of the periodic table, equivalent to the leading order terms of our didactic example. Second, we plot the difference between the smooth asymptotic curve and the QC data augmented by acRPA estimates to obtain a sense of the higher-order terms that determine shell structure along rows of the periodic table. We have already constructed such curves for correlation: $e_{AC}^{nob}(Z)$ fitting values for the noble gases using Eq. (54) and an analogous curve, $e_{AC}^{AE}(Z)$, for the alkali earths. As shown in Fig. 8, the two curves have the same behavior at large Z , but the AE curve is more reliable for lower Z , so we adopt the latter as standard.

To create smooth functions for exchange, we fit exchange energy results with continuous functions of Z and apply these functions for every value of Z . We standardize on alkali earths to be consistent with correlation. As we know LDA becomes relatively exact for exchange for large Z , we define

$$e_{AX} = E_X/Z - A_X Z^{2/3} \quad (71)$$

and fit EXX energies for alkali earths with

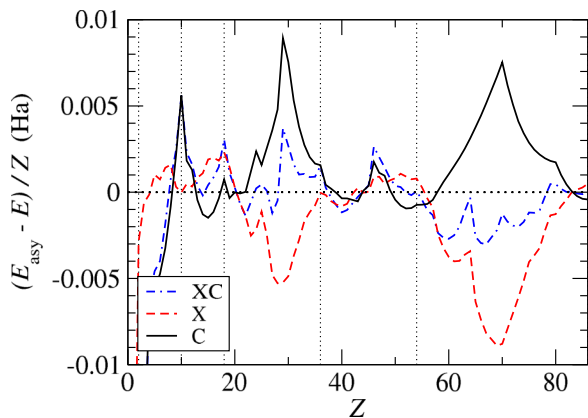


FIG. 10. Difference between the smooth asymptotic limiting functions for asymptotically corrected exchange and correlation energies and their QC values, versus atomic number. XC is exchange-correlation. Vertical lines denote location of noble gases to better visualize the location of periodic table rows.

$$e_{AX}^{\text{smooth}} = -(0.1466x^3 + 0.0314x^2 + 0.0823), \quad (72)$$

where $x = 1 - Z^{-1/3}$. This gives $B_X = -0.260$ in agreement with a previous estimate of -0.24 .²¹ The value of -0.08 at $Z = 1$ is somewhat off the actual value of -0.11 , but gives a close fit to e_{AX} for all $Z > 2$.

In Fig. 10, we plot the deviations of the exchange and correlation energies per electron from the smooth fits. This is where acRPA is important: To see the periodic pattern in the deviations in the correlation energy by including the large Z values. We have also included vertical lines at the noble gas atoms, to show the periodicity.

There are many interesting features in this plot.

- There is a clear (anti-)correlation between the correlation deviation and the exchange deviation, showing tremendous cancellation of “errors” in the separate components of the deviations. Thus, adding Eqs. (72) and $e_{AC}^{\text{AE}}(Z)$ yields a much more accurate estimate of XC than either separately. Shell structure is much greater in either exchange or correlation alone than in XC.
- The greatest deviations occur about the middle of the odd rows, and deviations are almost negligible throughout the 4th row.
- Filled angular momentum subshells tend to be marked by cusp-like behavior, especially for correlation. These are more apparent if the irregularities in filling for d and f subshells are ignored.
- We observe the pattern that whenever the most loosely bound electron also has the highest angular momentum, the deviation grows as that angular momentum subshell is filled and drops once the next subshell is filled. For example, for $Z = 21$ – 29 , the 3d-shell is being filled and the deviation grows and then drops rapidly as the 4p’s are filled. Note that this only happens when a given subshell is filled for the first time; there is little effect when the 4d’s are being filled. A similar pattern appears for the 4f’s and (to a lesser extent) even for the 2p’s.

IV. CONSEQUENCES

The majority of the numerical work in this manuscript has been devoted to the extraction of an accurate numerical estimate for B_C , which characterizes the leading correction to LDA correlation for atoms, and is strong evidence for the locality conjecture. In this section, we assume that conjecture is true and discuss its consequences for DFT approximations. We use the mathematical prolog and its relevance to the kinetic energy of non-interacting atoms to illustrate this, by discussing $T_S[n]$, $E_X[n]$, and $E_C[n]$.

A. Relevance of uniform gas to Coulombic matter

In the math prolog, we showed that, for the kinetic energy of non-interacting atoms,

$$T_S(Z) = (3/2)^{1/3} Z^{7/3} - Z^2/2 + \dots \quad (73)$$

For real atoms,

$$T_S(Z) = A_S Z^{7/3} - Z^2/2 + \dots, \quad (74)$$

where $A_S = 0.768\,745$ is given exactly by TF theory, while

$$E_X(Z) = -A_X Z^{5/3} + B_X Z + \dots \quad (75)$$

and

$$E_C(Z) = -A_C Z \ln Z + B_C Z + \dots \quad (76)$$

In every case, a local density approximation yields the leading term for large Z . Thus, LDA yields the exact large- Z limit of each component for *every* electronic system. It is a *universal* limit for all matter. The form and coefficients of local approximations can be most easily calculated from the uniform electron gas, but in principle can be extracted from taking any system, such as atoms, to the large- Z limit.

But note that correlation is different from exchange and the kinetic energy. In the latter two, the corrections to the dominant term are smaller by a factor of at least $Z^{-1/3}$. Thus the corrections are relatively small for $Z > 50$ and relatively easily identified. For correlation, the leading term is only $\ln Z$ larger, meaning Z must be vast before it dominates. Thus, lists of values of $E_C(Z)$ for $Z < 100$ *alone* cannot be used to extract this behavior accurately. Moreover, approximations (especially any designed only for lighter atoms) can ignore this contribution and still remain accurate. Moreover, since that term is determined by the high-density behavior of the uniform gas, and the next term in LDA is not accurate, all the rest of the correlation energy of the uniform gas is not particularly relevant to atomic correlation energies. Thus almost all popular approximations to E_X reduce to LDA for uniform densities, but not so for E_C .

Except for model 1-d systems,^{14–16,85,86} no one has ever written down a general functional approximation that recovers the leading corrections to LDA for all systems. The gradient expansion approximation does this for slowly varying densities, but then is quite incorrect for atoms.²¹ Generalized gradient approximations attempt to capture both, but find that they are irreconcilable.^{23,24}

B. Performance of semilocal approximations

The locality principle claims that one can understand the successes and failures of semilocal DFT in terms of the large- Z expansion. We now consider three basic properties often calculated with such approximations: ionization potentials, bond energies, and bond lengths. Note that all these depend only on energy differences, not the total energies studied here. But we argue below that the qualitative behavior of semilocal approximations for each of these cases can be understood in terms of the locality principle.

The simplest case is ionization energies, which can be studied for atoms.⁸⁷ Within the numerical accuracy, at the exchange level, LDA yields the exact ionization energy in the large- Z limit, and GGA (in the PBE case, at least) correctly reduces to LDA in this limit. This is consistent with the fact that GGA's and global hybrids do not typically yield significant improvement over LDA for ionization energies.^{7,88} An analogous result was found for XC: PBE corrections to LDA ionization energies are very small (or zero) in this limit. Thus, at least for atoms, LDA becomes relatively exact for ionization potentials in this limit, and our standard GGA's do not yield much improvement. They do not produce the leading correction in the asymptotic expansion for the ionization potential and so are not systematically better than LDA for real systems.

Next consider bond energies. GGA's typically improve atomization energies relative to LDA. Both PBE and B88 yield accurate asymptotic corrections to LDA exchange for large Z . Thus the corrections are accurate for both the equilibrium molecule and the isolated atoms, sufficiently so as to produce improved energy differences. This suggests that both cases are improved by improving the asymptotics.

But now consider what happens as a molecule is stretched relative to equilibrium. The molecular levels become nearly degenerate. The smaller the gap, the further they are away from the large- Z limit, which assumes a continuum of levels. To see this semiclassically, we note that the Coulson-Fisher point in LDA for H_2 is at $R = 3.3$ a.u.⁸⁹ If we consider the point where the HOMO level of the exact KS potential just touches the maximum in the KS potential well, this occurs at about the same distance.⁹⁰ As R increases through 3.3, the classical turning point surface of the KS potential at the HOMO energy is divided into two isolated regions. Thus the onset of strong static correlation coincides with a qualitative change in the nature of the semiclassical (i.e., local) approximation. The asymptotic expansion works well at equilibrium or for isolated atoms, but fails completely as 3.3 is approached, because of the degeneracy. This is the semiclassical explanation of the failure of semilocal approximations as bonds are stretched.

Finally, we discuss bond lengths, which are determined by the derivative of the binding energy curve at equilibrium. The asymptotic expansion in Z should work (almost) equally well for separations in and near equilibrium. The classical turning point structure at the HOMO level does not change qualitatively. Furthermore, the asymptotic behavior for large- Z remains the same for each value, and so irrelevant for the derivative. Exchange GGAs that capture the correct asymptotics of the total energy violate the gradient expansion,

which should be accurate for these small changes. This was (part of) the reasoning behind PBEsol, which restores the gradient expansion for exchange and improves lattice constants of many solids.²²

V. CONCLUSIONS

The central result of this paper is to combine existing numerical evidence for the correlation energy of non-relativistic atoms, together with knowledge of the asymptotic form for the dependence of this energy on Z , to extract the leading correction to the local density approximation for atoms in the large- Z limit. This is a key number that characterizes the leading error made by LDA, and that can be corrected by more sophisticated approximations. We have argued that this number is non-empirical and should be used as an exact condition for non-empirical construction of functionals.

In a preliminary report, we constructed a non-empirical GGA that was asymptotically correct for atoms.⁹¹ The method was then used to impose exact conditions on the SCAN meta-GGA.⁹²

ACKNOWLEDGMENTS

This work was supported by NSF Grant No. CHE-1464795. S.P. was supported by the European Community through the FP7's MC-IIF MODENADYNA, Grant Agreement No. 623413 and by the European Commission (Grant No. FP7-NMP-CRONOS). T.G. recognizes computing support from the Griffith University Gowonda HPC Cluster. We thank John Perdew and Raphael Ribeiro for many useful discussions and Eberhard Engel for the use of his atomic DFT code, OPMKS.

¹W. Kohn and L. J. Sham, *Phys. Rev.* **140**, A1133 (1965).

²A. Pribram-Jones, D. A. Gross, and K. Burke, *Annu. Rev. Phys. Chem.* **66**, 283–304 (2015).

³C. Fiolhais, F. Nogueira, and M. Marques, *A Primer in Density Functional Theory* (Springer-Verlag, New York, 2003).

⁴A. D. Becke, *Phys. Rev. A* **38**, 3098 (1988).

⁵C. Lee, W. Yang, and R. G. Parr, *Phys. Rev. B* **37**, 785 (1988).

⁶A. D. Becke, *J. Chem. Phys.* **98**, 5648 (1993).

⁷J. P. Perdew, J. A. Chevary, S. H. Vosko, K. A. Jackson, M. R. Pederson, D. J. Singh, and C. Fiolhais, *Phys. Rev. B* **46**, 6671 (1992).

⁸J. P. Perdew, K. Burke, and M. Ernzerhof, *Phys. Rev. Lett.* **77**, 3865 (1996); *ibid.* **78**, 1396(E) (1997).

⁹S. Kümmel and L. Kronik, *Rev. Mod. Phys.* **80**, 3 (2008).

¹⁰M. Dion, H. Rydberg, E. Schröder, D. C. Langreth, and B. I. Lundqvist, *Phys. Rev. Lett.* **92**, 246401 (2004).

¹¹M. Levy, *Proc. Natl. Acad. Sci. U. S. A.* **76**, 6062 (1979).

¹²E. H. Lieb, *Rev. Mod. Phys.* **53**, 603 (1981).

¹³E. H. Lieb and B. Simon, *Adv. Math.* **23**, 22 (1977).

¹⁴P. Elliott, D. Lee, A. Cangi, and K. Burke, *Phys. Rev. Lett.* **100**, 256406 (2008).

¹⁵P. Elliott, A. Cangi, S. Pittalis, E. K. U. Gross, and K. Burke, *Phys. Rev. A* **92**, 022513 (2015).

¹⁶R. F. Ribeiro, D. Lee, A. Cangi, P. Elliott, and K. Burke, *Phys. Rev. Lett.* **114**, 050401 (2015).

¹⁷J. Schwinger, *Phys. Rev. A* **22**, 1827 (1980).

¹⁸J. Schwinger, *Phys. Rev. A* **24**, 2353 (1981).

¹⁹J. Conlon, *Commun. Math. Phys.* **88**, 133 (1983).

²⁰C. Fefferman and L. Seco, *Adv. Math.* **107**, 1 (1994).

²¹P. Elliott and K. Burke, *Can. J. Chem.* **87**, 1485 (2009).

²²J. P. Perdew, A. Ruzsinszky, G. I. Csonka, O. A. Vydrov, G. E. Scuseria, L. A. Constantin, X. Zhou, and K. Burke, *Phys. Rev. Lett.* **100**, 136406 (2008).

- ²³Y. Zhang and W. Yang, *Phys. Rev. Lett.* **80**, 890 (1998).
- ²⁴J. Perdew, K. Burke, and M. Ernzerhof, *Phys. Rev. Lett.* **80**, 891 (1998).
- ²⁵L. A. Constantin, A. Terentjevs, F. Della Sala, P. Cortona, and E. Fabiano, *Phys. Rev. B* **93**, 045126 (2016).
- ²⁶S. Laricchia, E. Fabiano, L. A. Constantin, and F. D. Sala, *J. Chem. Theory Comput.* **7**, 2439 (2011).
- ²⁷L. A. Constantin, E. Fabiano, S. Laricchia, and F. Della Sala, *Phys. Rev. Lett.* **106**, 186406 (2011).
- ²⁸S. P. McCarthy and A. J. Thakkar, *J. Chem. Phys.* **134**, 044102 (2011).
- ²⁹H. Kunz and R. Rueedi, *Phys. Rev. A* **81**, 032122 (2010).
- ³⁰E. Clementi and G. Corongiu, *Int. J. Quantum Chem.* **62**, 571 (1997).
- ³¹The values reported for A_C and B_C on pages 9 and 10 of Ref. 29 appear to have typographical errors. To reproduce Fig. 1, we divide their A_C by three and reverse the sign of B_C . But even with these corrections, the resulting value for B_C is inaccurate.
- ³²B.-G. Englert, *Semiclassical Theory of Atoms*, Lecture Notes in Physics Vol. 300 (Springer Verlag, Berlin, 1988).
- ³³P. Hohenberg and W. Kohn, *Phys. Rev.* **136**, B864 (1964).
- ³⁴L. H. Thomas, *Math. Proc. Cambridge Philos. Soc.* **23**, 542 (1927).
- ³⁵E. Fermi, *Z. Physik* **48**, 73 (1928).
- ³⁶L. Spruch, *Rev. Mod. Phys.* **63**, 151 (1991).
- ³⁷D. Lee, L. A. Constantin, J. P. Perdew, and K. Burke, *J. Chem. Phys.* **130**, 034107 (2009).
- ³⁸U. von Barth and L. Hedin, *J. Phys. C: Solid State Phys.* **5**, 1629 (1972).
- ³⁹D. M. Ceperley and B. J. Alder, *Phys. Rev. Lett.* **45**, 566 (1980).
- ⁴⁰S. H. Vosko, L. Wilk, and M. Nusair, *Can. J. Phys.* **58**, 1200 (1980).
- ⁴¹J. P. Perdew and Y. Wang, *Phys. Rev. B* **45**, 13244 (1992).
- ⁴²R. Jones and O. Gunnarsson, *Rev. Mod. Phys.* **61**, 689 (1989).
- ⁴³R. O. Jones, *Rev. Mod. Phys.* **87**, 897 (2015).
- ⁴⁴R. M. Dreizler and E. K. U. Gross, *Density Functional Theory: An Approach to the Quantum Many-Body Problem* (Springer-Verlag, Berlin, 1990).
- ⁴⁵L. Kleinman and S. Lee, *Phys. Rev. B* **37**, 4634 (1988).
- ⁴⁶S.-K. Ma and K. Brueckner, *Phys. Rev.* **165**, 18 (1968).
- ⁴⁷D. Langreth and J. Perdew, *Phys. Rev. B* **15**, 2884 (1977).
- ⁴⁸A. D. Becke, *J. Chem. Phys.* **140**, 18A301 (2014).
- ⁴⁹E. Engel and R. M. Dreizler, *Density Functional Theory: An Advanced Course* (Springer, Berlin, 2011).
- ⁵⁰A. Görling and M. Ernzerhof, *Phys. Rev. A* **51**, 4501 (1995).
- ⁵¹M. Levy and J. Perdew, *Phys. Rev. A* **32**, 2010 (1985).
- ⁵²J. Harris and R. Jones, *J. Phys. F* **4**, 1170 (1974).
- ⁵³D. Langreth and J. Perdew, *Solid State Commun.* **17**, 1425 (1975).
- ⁵⁴O. Gunnarsson and B. Lundqvist, *Phys. Rev. B* **13**, 4274 (1976).
- ⁵⁵E. Lieb and B. Simon, *Phys. Rev. Lett.* **31**, 681 (1973).
- ⁵⁶S. Fournais, M. Lewin, and J. P. Solovej, e-prints [arXiv:1510.01124](https://arxiv.org/abs/1510.01124) [math-ph] (2015).
- ⁵⁷O. J. Heilmann and E. H. Lieb, *Phys. Rev. A* **52**, 3628 (1995).
- ⁵⁸J. Scott, *Philos. Mag.* **43**, 859 (1952).
- ⁵⁹Z. Levine and P. Soven, *Phys. Rev. Lett.* **50**, 2074 (1983).
- ⁶⁰B.-G. Englert and J. Schwinger, *Phys. Rev. A* **26**, 2322 (1982).
- ⁶¹B.-G. Englert and J. Schwinger, *Phys. Rev. A* **29**, 2339 (1984).
- ⁶²B.-G. Englert and J. Schwinger, *Phys. Rev. A* **29**, 2353 (1984).
- ⁶³B.-G. Englert and J. Schwinger, *Phys. Rev. A* **29**, 2331 (1984).
- ⁶⁴B.-G. Englert and J. Schwinger, *Phys. Rev. A* **32**, 26 (1985).
- ⁶⁵B.-G. Englert and J. Schwinger, *Phys. Rev. A* **32**, 36 (1985).
- ⁶⁶B.-G. Englert and J. Schwinger, *Phys. Rev. A* **32**, 47 (1985).
- ⁶⁷J. P. Perdew, L. A. Constantin, E. Sagvolden, and K. Burke, *Phys. Rev. Lett.* **97**, 223002 (2006).
- ⁶⁸K. Burke, M. Ernzerhof, and J. P. Perdew, *Chem. Phys. Lett.* **265**, 115 (1997).
- ⁶⁹S. P. McCarthy and A. J. Thakkar, *J. Chem. Phys.* **136**, 054107 (2012).
- ⁷⁰S. J. Chakravorty, S. R. Gwaltney, E. R. Davidson, F. A. Parpia, and C. F. p Fischer, *Phys. Rev. A* **47**, 3649 (1993).
- ⁷¹H. Eshuis, J. Bates, and F. Furche, *Theor. Chem. Acc.* **131**, 1 (2012).
- ⁷²S. Lebègue, J. Harl, T. Gould, J. G. Ángyán, G. Kresse, and J. F. Dobson, *Phys. Rev. Lett.* **105**, 196401 (2010).
- ⁷³T. Björkman, A. Gulans, A. V. Krashenninnikov, and R. M. Nieminen, *J. Phys.: Condens. Matter* **24**, 424218 (2012).
- ⁷⁴T. Gould and J. F. Dobson, *J. Chem. Phys.* **138**, 014103 (2013).
- ⁷⁵T. Gould and J. F. Dobson, *J. Chem. Phys.* **138**, 014109 (2013).
- ⁷⁶T. Gould and J. Toulouse, *Phys. Rev. A* **90**, 050502 (2014).
- ⁷⁷S. Chakravorty and E. Davidson, *J. Phys. Chem.* **100**, 6167 (1996).
- ⁷⁸M. Gell-Mann and K. Brueckner, *Phys. Rev.* **106**, 364 (1957).
- ⁷⁹L. Onsager, L. Mittag, and M. J. Stephen, *Ann. Phys. (Leipzig)* **473**, 71–77 (1966).
- ⁸⁰This may be derived from a least squares fit to a cubic polynomial of the nuclear charge Z as a function of n_{HOMO} for the noble gas atoms. This is inverted to an expression $n_{\text{HOMO}}(Z)$ whose coefficients are integers nearly within fitting error.
- ⁸¹J. E. Bates and F. Furche, *J. Chem. Phys.* **139**, 171103 (2013).
- ⁸²S. Kurth and J. P. Perdew, *Phys. Rev. B* **59**, 10461 (1999).
- ⁸³Z. Yan, J. P. Perdew, S. Kurth, C. Fiolhais, and L. Almeida, *Phys. Rev. B* **61**, 2595 (2000).
- ⁸⁴Additional numerical tests suggest that our RPA energies may be systematically over-estimated, which would reduce the discrepancy between theory and our calculations. However, as these possible systematic errors lie within the overall numerical error bars we do not attempt to correct for them.
- ⁸⁵A. Cangi, D. Lee, P. Elliott, and K. Burke, *Phys. Rev. B* **81**, 235128 (2010).
- ⁸⁶A. Cangi, D. Lee, P. Elliott, K. Burke, and E. K. U. Gross, *Phys. Rev. Lett.* **106**, 236404 (2011).
- ⁸⁷L. A. Constantin, J. C. Snyder, J. P. Perdew, and K. Burke, *J. Chem. Phys.* **133**, 241103 (2010).
- ⁸⁸G. I. Csonka, J. P. Perdew, and A. Ruzsinszky, *J. Chem. Theory Comput.* **6**, 3688 (2010).
- ⁸⁹R. A. R. Bauernschmitt, *Chem. Phys. Lett.* **256**, 454 (1996).
- ⁹⁰M. A. Buijse, E. J. Baerends, and J. G. Snijders, *Phys. Rev. A* **40**, 4190 (1989).
- ⁹¹K. Burke, A. Cancio, T. Gould, and S. Pittalis e-print [arXiv:1409.4834v1](https://arxiv.org/abs/1409.4834v1) (submitted).
- ⁹²J. Sun, A. Ruzsinszky, and J. P. Perdew, *Phys. Rev. Lett.* **115**, 036402 (2015).